

# Qualitative and quantitative detection of Sudan I and II adulterated in chili powders by front-face synchronous fluorescence spectroscopy

## Aggregation-induced emission in solid food

Zhao-Xi Liu

Tianjin University of Commerce

Jin Tan (✉ [tanjin@tjcu.edu.cn](mailto:tanjin@tjcu.edu.cn))

Tianjin University of Commerce

---

### Research Article

**Keywords:** Sudan dye, Chili powder, Aggregation-induced emission (AIE), Front-face synchronous fluorescence spectroscopy (FFSFS), Principal component analysis – linear discriminant analysis (PCA–LDA), Partial least square regression (PLSR)

**Posted Date:** April 15th, 2022

**DOI:** <https://doi.org/10.21203/rs.3.rs-1539582/v1>

**License:** © ⓘ This work is licensed under a Creative Commons Attribution 4.0 International License.

[Read Full License](#)

---

# Abstract

Sudan dyes are commonly found adulterants in chili related products. In this work, the unusual fluorescent behaviors of Sudan I and II in solid state were observed for the first time which are attributed to aggregation-induced emission (AIE). Taking advantage of their solid-state AIE properties, front-face synchronous fluorescence spectroscopy (FFSFS) was applied for the rapid and non-destructive determination of Sudan I or II in chili powders. For each dye, 90 adulterated chili powders containing 1–50 mg/g Sudan I or II were prepared. Qualitative and quantitative analyses were achieved by principal component analysis – linear discriminant analysis (PCA–LDA) and partial least square regression (PLSR), respectively. The built models were validated by full cross-validation, five-fold cross-validation and external validation. The sensitivity and specificity in discrimination were both 100%. For PLSR prediction, the coefficients of determination ( $R^2$ ) were greater than 0.96. The relative errors of prediction (REP) were 15.2% and 11.6% for Sudan I and II, respectively. AIE-based FFSFS offers a new route for the application of fluorescence spectroscopy in food authentication.

## 1 Introduction

As an old analytical technique with a long history, fluorescence spectroscopy is renowned for its high sensitivity, selectivity and simplicity. However, conventional right-angle fluorescence spectroscopy is not suitable for the direct measurement of concentrated liquid or solid samples due to the primary and secondary inner filter effects encountered in strongly absorbing matrices [1]. In these cases, solution by a solvent or a proper dilution is prerequisite. To deal with such samples, front-face fluorescence spectroscopy (FFFS) provides a convenient alternative. It measures the fluorescent excitation and emission on the frontal surface of sample, reflects the intrinsic fluorescence of bulk and opaque samples, and is hence particularly suitable for food samples [1]. It has been demonstrated to be a powerful tool for the rapid and non-destructive authentication of various kinds of foods and beverages [2–13].

Aggregation-induced emission (AIE) has been attracting numerous and continuous attentions since its proposal [14], especially in the past decade [15–17]. As an unusual fluorescence phenomenon, it is described to be a photophysical effect that fluorescent emission is induced by aggregate formation, either in solution state or in solid state [14]. In contrast to the commonly known aggregation-caused quenching (ACQ), it provides a new platform for the understanding of the underlying mechanisms of fluorophores in aggregate state and opens a new gate for a wide variety of technological applications including chemical sensing, bioimaging and therapeutics [15, 17]. In recent years, AIE-based sensors or probes have also been applied to food analysis [18–20]. However, the investigation of the AIE behaviors of the intrinsic components in solid foods is very scarce.

Sudan dyes (Fig. 1) are the most frequently found contaminants in chili related products [21]. They are illegally added to strengthen the bright red color of chilies. Although chromatographic techniques are competent to detect Sudan dyes accurately and sensitively, such analysis can prove tedious and cumbersome [22]. Compared with chromatographic methods, spectroscopic techniques can afford

simple, rapid and non-destructive measurements. Several kinds of spectroscopic methods have been developed to detect Sudan dyes in foods [23–33]. In this field, Di Anibal and coworkers have developed many methods via UV-visible, near infrared (NIR), Raman and nuclear magnetic resonance (NMR) spectroscopies [23–26, 33]. They also used synchronous fluorescence spectroscopy to construct a screening method for the adulteration of chili samples with Sudan I [27]. In this work, traditional right-angle geometry was adopted and Sudan I needed to be extracted from sample by isopropyl alcohol. Besides, they mainly focused on the qualitative discrimination of unadulterated and adulterated samples, without quantitative intent. In another work, Monago-Maraña et al. employed fiber optic probe to achieve non-destructive fluorescent detection of Sudan I in paprika powder [31]. They found partial least squares regression (PLSR) based on first-order emission spectra gave poor validation results while second-order algorithms significantly improved the model robustness. The authors attributed the large errors to the naturally varied color of paprika that could influence the Sudan I fluorescence signal. Though excellent results were obtained in this work, the authors stated that it would be better if the method were proven also competent for classification of adulterated or unadulterated samples. Furthermore, as their method is limited to Sudan I, the possibility of quantifying other Sudan dyes is worthy of investigation.

The unusual fluorescence of Sudan I has been observed and explored for its cell imaging applications [34]. The AIE mechanism of Sudan I in solution state has been proven, however, its AIE behavior in solid state has not been investigated and utilized. Herein, we will take the Sudan dyes and chili powders as the example to investigate the AIE phenomenon in solid foods and try to take advantage of such unique characteristic to propose an FFS-based method for the rapid and non-destructive determination of Sudan dyes in chili powders both qualitatively and quantitatively. To eliminate the matrix interference from naturally varied color of chili powders, synchronous fluorescence is employed. Different from the conventional excitation–emission scan, the synchronous scanning mode can largely eliminate the interference, clean the spectra and sharpen the band. It has been widely used for various kinds of food authentication [2, 6–7, 13, 27, 35–37]. In this work, the advantage of synchronous fluorescence spectroscopy is utilized to eliminate the matrix interference and the feasibility of using a simple algorithm to identify multiple Sudan dyes will be studied. The goal of this study is to develop a simple, rapid and non-destructive method for the qualitative and quantitative authentication of Sudan dye adulteration in chili powders by combining the advantage of AIE and front-face synchronous fluorescence spectroscopy (FFSFS), providing an alternative procedure to guarantee consumers' right and food safety.

## 2 Materials And Methods

### 2.1 Materials

All reagents used were of at least analytical grade. Ultrapure water was used throughout the experiments. Acetonitrile (MeCN) of high performance liquid chromatography (HPLC)-grade was obtained from Kermel Chemical Reagent Co., Ltd. (Tianjin, China). Barium sulfate ( $\text{BaSO}_4$ ) was bought from Guangfu Fine Chemical Reagent Co., Ltd. (Tianjin, China). Sudan I, II, III and IV were purchased from Aladdin Reagent

Co., Ltd. (Shanghai, China). All solutions were filtered through 0.45  $\mu\text{m}$  membrane filters or syringe filters (Shanghai Milimo Separation Technology Co., Ltd.) prior to HPLC.

## 2.2 Samples

Nine commercial brands of chili powder were purchased from JD.com global online shopping site. To reflect natural variations and enlarge matrix interferences, those samples showing a wide variability in color were selected as representative. Three bottles were collected for each brand. They were kept at 4  $^{\circ}\text{C}$  in the dark and guaranteed not to past their expiration date prior to analysis. All these chili powder samples were tested by HPLC to be free of any Sudan dye. The HPLC and fluorescent analyses of the same sample were performed in tandem within one day to avoid any change of the analytes. Prior to analysis, chili powders were ground, sieved and oven-dried at 105  $^{\circ}\text{C}$  for 8 h, and those dried fine powders with particle size in the range of 0.096–0.2 mm were collected for further analysis. Since commercial Sudan I contained a portion of moisture, it was also dried at 105  $^{\circ}\text{C}$  for 8 h and kept in a desiccator prior to use.

Adulterated chili powder samples were prepared by adding an amount of Sudan I or II to each brand of chili powder in the range of 1–5 mg/g with a step of 1 mg/g (0.1–0.5%, w%), and in the range of 10–50 mg/g with an interval of 10 mg/g (1–5%, w%). Thus, for each dye, 90 adulterated chili powder samples were obtained (9 brands  $\times$  10 concentrations). Specifically, appropriate weights of the adulterant and chili powder were mixed and shaken adequately to make the mixture homogenous. Besides, the solid solution of Sudan I and II in a fluorescent inert solid,  $\text{BaSO}_4$ , were also prepared analogously at the same concentration levels as the adulterated chili powders.

## 2.3 HPLC analysis

HPLC analysis was carried out with an Agilent 1260 system (Agilent, Palo Alto, CA, USA) consisting of a quaternary pump (G7111A), a diode array detector (G7115A) and an autosampler (G7129A) with a 20  $\mu\text{L}$  sample loop. An Alltima-C18 column (250 mm  $\times$  4.6 mm I.D., 5  $\mu\text{m}$ , Grace, Columbia, MD, USA) was used for chromatographic separation.

The simultaneous analysis of four Sudan dyes was performed according to a literature method [22] with a slight modification. The mobile phase was acetonitrile-water (98:2, v:v). The flow rate was set at 1.0 mL/min. The column temperature was fixed at 30 $^{\circ}\text{C}$ . The injection volume was 20  $\mu\text{L}$  and the detector was set at 478 (Sudan I), 496 (II), 510 (III) and 520 (IV) nm. For sample preparation, 100 mg of dried sample was homogenized with 20 mL of acetonitrile and vigorously shaken and ultrasonicated for 40 min. After centrifugation at 3000 rpm for 5 min, the supernatant was filtered through a 0.45  $\mu\text{m}$  syringe filter. The HPLC method was validated by repeatability, reproducibility and recovery test. The detection limits ( $3\sigma$ ) for four Sudan dyes in chili powder were 0.4  $\mu\text{g/g}$ . All the chili powder samples were detected by HPLC, and the results showed that none of four Sudan dye was beyond the detection limit in the samples. The actual contents of Sudan I or II in all the adulterated chili powders were also determined as references.

## 2.4 FFSFS measurement

Fluorescence spectra were acquired with an FS5 spectrofluorometer (Edinburgh, Livingston, Scotland, Britain) with a 150 W xenon lamp source for excitation. The slit widths for excitation and emission were both 2 nm. The front-face geometry of chili powders was used for the spectra acquisition with an SC-10 front-face sample holder at room temperature (25°C). Sixty milligram of samples was mounted in the sample holder. The incidence angle of the excitation radiation was 30° which was fixed by the sample holder. The excitation and emission were scanned simultaneously, and the  $\lambda_{\text{ex}}$  was in the 250–600 nm range with a step of 1 nm. The constant wavelength interval ( $\Delta\lambda$ ) between  $\lambda_{\text{ex}}$  and emission wavelength ( $\lambda_{\text{em}}$ ) was set at 30–300 nm with a step of 10 nm. Fluorescence intensities were plotted as a function of  $\lambda_{\text{ex}}$ . For each sample three spectra were measured successively and the average of the three measurements was used for further analysis. The relative standard deviation (RSD) of three replicate samples of the same brand was calculated to assess the in-group measurement precision.

## 2.5 Statistical analysis

Prior to statistical analysis, several spectral data pretreatments including normalization, standard normal variate (SNV), multiplicative scatter correction (MSC), first (1st) and second (2nd) derivative preprocesses were tested. Principal component analysis (PCA) and linear discriminant analysis (LDA) were performed using IBM SPSS 19.0 (IBM, USA). PLSR was executed by Unscrambler X 10.4 (CAMO Oslo, Norway). PCA followed by LDA was used to discriminate the unadulterated and adulterated chili powders. PLSR models was then constructed to predict the content of adulterant. Both the qualitative and quantitative models were optimized and validated by full (*leave-one-out*) cross-validation, five-fold cross-validation and external validation. The spectra used for all the analyses are the synchronous fluorescence data at a certain  $\Delta\lambda$  with  $\lambda_{\text{ex}}$  from 250 to 600 nm, thus the total variable number for one  $\Delta\lambda$  is 351. Both the spectra data pretreatment and the selection of  $\Delta\lambda$  were carefully optimized. For PCA, all the 207 samples (27 unadulterated chili powders (9 brands  $\times$  3 bottles) + 90 chili powders adulterated with Sudan I + 90 chili powders adulterated with Sudan II) were analyzed. After that, LDA was performed to derive a classification rule according to unadulterated / adulterated with Sudan I / adulterated with Sudan II based on the obtained PCs scores with eigen values larger than 1. For PLSR, 90 adulterated samples composed the calibration set for each dye. The corresponding root mean square error of calibration (RMSEC), coefficient of determination for calibration ( $R^2_{\text{c}}$ ), root mean square error of cross-validation (RMSECV) and coefficient of determination for cross-validation ( $R^2_{\text{cv}}$ ) were calculated. The optimal number of PLSR latent variables was decided by plotting the RMSECV versus the number of components and determining the minimum of the plot. For external validation, the 90 samples were sorted by the adulterant concentration, and every five sample was injected into the test set ( $n = 18$ ). The remaining samples composed the training set ( $n = 72$ ). The test set was then used to evaluate the predictive ability of the built models. Root mean square error of prediction (RMSEP) and the corresponding coefficient of determination for prediction ( $R^2_{\text{p}}$ ) were determined. The relative error of prediction (REP) was calculated as percentage ratio of the RMSEP to the mean of the actual content values. The standard error of

prediction (SEP) and residual predictive deviation (RPD) which is the ratio of the standard deviation of reference values to RMSEP, were also determined.

## 3 Results And Discussions

### 3.1 AIE behaviors of Sudan dyes in solid state

As the AIE mechanism of Sudan I in solution has already been revealed by Yoon et al. [34], the AIE behaviors of Sudan I and its analogue Sudan II in solution state were not repeatedly examined. Instead, the FFSFS of Sudan I and II in pure solid state were first scanned. As presented in Fig. 2 and Fig. 3, both the two dyes showed unusual broad-band fluorescence excitations which can be observed in the whole tested range ( $\lambda_{\text{ex}} = 250\text{--}600\text{ nm}$ ). As the maximal  $\lambda_{\text{em}}$  remains constant at ca. 600 nm, the synchronous fluorescent contour plots display a regular shape of long strip, with the  $\Delta\lambda$  ranging from 30 to 300 nm. Conventional fluorophores are generally non-fluorescent in solid state, known as ACQ. However, Sudan I and II show relatively strong fluorescence in their solid state. Actually, it has been confirmed by Yoon et al. that Sudan I has a typical AIE behavior [34]. They found *o*-phenylazonaphthol compounds had a higher fluorescence intensity in their solid states than in solution states. Owing the same *o*-phenylazonaphthol skeleton as Sudan I, Sudan II exhibits a similar AIE behavior in solid state. The locations of the fluorescent bands are analogous to those of Sudan I. However, its fluorescence is significantly stronger than that of Sudan I (ca. 2-folds as Sudan I at maximal  $\lambda_{\text{ex}}$ ). Except the fluorescence quantum yield, another slight difference exists in their contour plots. For Sudan I, the relatively shorter wavelength excitations ( $\lambda_{\text{ex}} = 300\text{--}400\text{ nm}$  and  $\Delta\lambda = 200\text{--}300\text{ nm}$ ) yield much stronger emission than the longer ones ( $\lambda_{\text{ex}} = 500\text{--}600\text{ nm}$  and  $\Delta\lambda = 30\text{--}100\text{ nm}$ ). However, for Sudan II, the above-mentioned two ranges show parallel intensities. Such difference between the two dyes gives the result that Sudan II is even more intensive by long wavelength excitation. This difference may provide the feasibility to distinguish Sudan I and II in chili powders. The relationship between such spectral distinction and the structural difference existing between the two dyes, i.e., two substituted methyl moieties in *o*-phenylazonaphthol skeleton of Sudan II, needs further investigation.

The AIE mechanism of Sudan I and II in solid state can be the restriction of intramolecular motions (RIM) [38]. In a typical ACQ process, the strong  $\pi\text{--}\pi$  stacking interactions between the fluorophores normally results in the fluorescence quenching. While in AIE, the RIM blocks the non-radiative route and re-opens the radiative gate [38]. The large Stokes shift ( $\Delta\lambda = 200\text{--}300\text{ nm}$ ) indicates the formation of intramolecular hydrogen bonds and the consequent excited state intramolecular proton transfer (ESIPT) which lowers the energy of excited state and increases the energy loss between the excitation and the emission [39].

Except the spectral difference between Sudan I and II, another physical difference was found. Drying method showed that the commercial Sudan I used in this work had ca. 30% moisture. While after the loss of 30% moisture by drying treatment, the fluorescent intensity of Sudan I nearly doubled, indicating that the moisture does not only decrease the fluorescence solely by the occupation of weight. Besides, Sudan I

with higher moisture tended to suffer from larger measurement errors. Therefore, it was dried at 105 °C for 8 h and kept in a desiccator prior to use in the present study.

The FFSFS properties of Sudan III and IV in solid state were also tested. It is interesting that they have no fluorescence emission in the tested range. Compared with Sudan I and II, Sudan III and IV possess an additional phenylazo moiety (Fig. 1). The reason why Sudan III and IV do not show an AIE behavior in solid state may be related to the ineffective RIM process and the following  $\pi$ - $\pi$  stacking interactions due to the second phenylazo moiety, which deserves further investigation.

## 3.2 AIE behaviors of Sudan dyes in solid solutions

To further investigate the AIE behaviors of Sudan I and II in solid solutions, their dilutions in a fluorescent inert reagent BaSO<sub>4</sub> were prepared. Sudan I and II again exhibit different trends with the increase of concentration. As illustrated in Fig. 2, the noticeable characteristic emissions of Sudan I appear in the spectra when the concentration increases to 1%, and then gradually strengthens along with the further increase of concentration. However, such increase is not linear with the concentration. Besides, the long wavelength excitation centered at  $\lambda_{\text{ex}} = 560$  nm and  $\Delta\lambda = 40$  nm is more obvious than the shorter ones. This is opposite to the observation of pure Sudan I in solid state, indicating the intermolecular distance has different effects on the short and long wavelength excitations in Sudan I's AIE. On the other hand, the situation is different for Sudan II (Fig. 3). The relatively shorter wavelength excitations ( $\lambda_{\text{ex}} = 300$ – $400$  nm and  $\Delta\lambda = 200$ – $300$  nm) and the longer ones ( $\lambda_{\text{ex}} = 550$ – $600$  nm and  $\Delta\lambda = 30$ – $100$  nm) emerge together when the concentration increases to 0.5% and then become stronger simultaneously. Once again, compared with Sudan I, Sudan II shows higher intensity at the same concentration and is easier to identify at lower concentrations.

## 3.3 FFSFS properties of chili powders

The FFSFS properties of chili powders were then investigated. The moisture and particle size were found to play important roles on the FFSFS intensity and measurement error. To enlarge the sensitivity and to reduce the error as much as possible, chili powders were oven-dried and sieved to yield dried fine powders. All the collected chili powders show similar overall shape in total synchronous fluorescence spectra, but the intensities of different bands can vary. Figure 4a-4c present the typical contour maps of three brands of chili powders. An obvious fluorescence peak appears at  $\lambda_{\text{ex}} = 420$  nm and  $\Delta\lambda = 260$  nm which should be ascribed to the low quantity of chlorophyll [12, 40]. Meanwhile, there are strong fluorescence emissions above  $\lambda_{\text{ex}} 500$  nm in the  $\Delta\lambda$  range of 30–150 nm. These composite emissions can be attributed to the carotenoids such as capsanthin, a natural pigment in chili pepper [40]. Owing to natural variation, these natural compounds show different profiles, making the red color of sample varying from pale to deep [40]. Nevertheless, all the fluorescence emissions of these natural components in chili powder are distinct from those of Sudan dyes without severe overlap.

The general tendency in total synchronous FFSFS spectra of increasing concentrations of Sudan I or II in chili powders is analogous to that in BaSO<sub>4</sub>. When the concentrations are higher than 1%, the

characteristic bands of Sudan dyes can be easily discerned even by the naked eye (Fig. 4d and 4e). Slight differences can be observed for Sudan I and II at the same  $\Delta\lambda$ , making the samples adulterated with the two dyes distinguishable.

### 3.4 Qualitative discrimination by PCA–LDA

To reduce the dimensionality of spectral data and to visualize the fluorescent fingerprints more clearly, PCA was first applied to the synchronous fluorescence spectral data. As only a simple algorithm was employed in this work, the influence of  $\Delta\lambda$  on the discrimination was carefully examined. After optimization, the selected  $\Delta\lambda$  for qualitative discrimination is 180 nm, while the optimal spectral data pretreatment method is smoothing by the Savitzky and Golay method followed by 1st derivative preprocess. Figure 5a shows the obtained two dimensional PCA score plot. The first two principal components account for 89.3% of the original variance. In this plot, a portion of the chili powders adulterated with 0.1–5% Sudan II are preliminarily separated from others while most of the chili powders adulterated with Sudan I are severely overlapped with the unadulterated ones, especially for certain brands of sample at lower adulterant concentrations.

As PCA is an unsupervised pattern recognition method, the discrimination task was then executed by the unsupervised LDA based on the obtained PCA scores. As can be seen from Fig. 5b, the three classes are completely isolated from each other. The sensitivity and specificity in all the cross- and external validation are 100%, i.e., no mis-classification has been made.

### 3.5 Quantitative prediction by PLSR

After the qualitative discrimination by PCA–LDA, the concentration of the adulterated Sudan I or II in chili powder was determined by PLSR. The optimal data pretreatment is smoothing by the Savitzky and Golay method followed by normalization, and different  $\Delta\lambda$  is selected for Sudan I and II. Table 1 shows the PLSR parameters in calibration, cross-validation and external validation. The  $R^2$  values are in the range of 0.963–0.987, and all the RMSE are no more than 0.4%. The REP are 15.2% and 11.6% for Sudan I and II, respectively. The corresponding RPD are 6.8 and 9.1, respectively. Although limited to the high concentration range, these results are acceptable, demonstrating that this simple algorithm is competent for the rough estimation of Sudan I or II at relatively high concentrations.

Table 1  
 PLSR statistics for determination of Sudan I and II (0.1 – 5%, w%)  
 in chili powders using front-face synchronous fluorescence  
 spectra at the optimal  $\Delta\lambda$  with  $\lambda_{ex}$  from 250 to 600 nm (the  
 variable number is 351).

parameter	Sudan I	Sudan II
$\Delta\lambda$ (nm)	80	230
No. of LV <sup>a</sup>	7	3
$R^2_c$ <sup>b</sup>	0.973	0.982
RMSEC <sup>c</sup>	0.27	0.23
$R^2_{cvf}$ <sup>d</sup>	0.963	0.979
RMSECV <sub>f</sub> <sup>e</sup>	0.32	0.25
$R^2_{cv5}$ <sup>f</sup>	0.968	0.980
RMSECV <sub>5</sub> <sup>g</sup>	0.30	0.25
$R^2_p$ <sup>h</sup>	0.977	0.987
RMSEP <sup>i</sup>	0.26	0.19
REP (%) <sup>j</sup>	15.2	11.6
prediction bias	0.05	0.06
SEP <sup>k</sup>	0.26	0.18
RPD <sup>l</sup>	6.8	9.1
<sup>a</sup> No. of LV, number of latent variables.		
<sup>b</sup> $R^2_c$ , determination coefficient of calibration.		
<sup>c</sup> RMSEC, root mean square error of calibration.		
<sup>d</sup> $R^2_{cvf}$ , determination coefficient of full cross-validation.		
<sup>e</sup> RMSECV <sub>f</sub> , root mean square error of full cross-validation.		
<sup>f</sup> $R^2_{cv5}$ , determination coefficient of 5-fold cross-validation.		

parameter	Sudan I	Sudan II
<sup>g</sup> RMSECV <sub>5</sub> , root mean square error of 5-fold cross-validation.		
<sup>h</sup> $R^2_p$ , determination coefficient of prediction.		
<sup>i</sup> RMSEP, root mean square error of prediction.		
<sup>j</sup> REP (%), relative error of prediction.		
<sup>k</sup> SEP, standard error of prediction.		
<sup>l</sup> RPD, ratio of the SD of reference values to RMSEP.		

The PLSR prediction result of Sudan I is not as good as that of Sudan II, with smaller  $R^2$  and RPD but larger RMSE and REP. As can be seen from Fig. 6, relatively large errors are presented in both low (0.1–0.5%) and high (1–5%) concentration levels. Such result should be highly related to the difference in fluorescence quantum yield between the two dyes. The fluorescent intensity of Sudan II is ca. 5-fold as that of Sudan I at the same concentration under the optimal conditions. The relatively lower fluorescence quantum yield of Sudan I makes the measurement hard to be sensitive and precise. Besides, as aforementioned, Sudan I may contain a portion of moisture which could significantly decrease its FFSFS intensity and enlarge the measurement error. Although all the samples were dried prior to test, owing to the presence of Sudan I, the moisture in the tested samples could not be strictly controlled to the same level. This may be the secondary reason for the inferior result of Sudan I.

The  $R^2$  and RMSE values of the present models are comparable with those of vibrational spectroscopic methods such as NIR and Raman [28]. Though still not that good as the second-order calibration, the proposed method is competitive compared with the first-order calibration reported by Monago-Maraña et al. [31]. Furthermore, both qualitative and quantitative analyses toward two Sudan dyes are demonstrated to be feasible. However, restricted by the AIE mechanism and low fluorescence quantum yield of Sudan dyes, the proposed method can only be used as a preliminary screening method for chili powders of large quantity adulteration.

In real applications, the concerns about how the detection can be affected by the presence of other compounds/contaminants existing in real-world samples should be addressed. Thanks to the high selectivity of fluorescence spectroscopy with the further enhanced specificity in solid state, the AIE ineffective Sudan III and IV do not make any interference to the detection of Sudan I or II, similarly are other non-fluorescent co-existing compounds/contaminants. Several fluorescent components in chili powders, including chlorophyll and capsanthin, have also been confirmed to be non-interfering. Besides, the experiments have also been performed in numerous replicates in different days, months and seasons. The results showed that the repeatability and reproducibility RSDs were all no more than 15%. Thus the detection is not significantly affected by variations in environmental temperature and humidity, both of

which are likely to vary substantially in broadly applicable screening methods. Of course, the samples need to be dried and sieved prior to test to enhance the sensitivity and decrease the measurement error. Finally, as the FFSFS spectra of Sudan I and II may resemble each other in the same region at different concentrations, the simultaneous analysis of the co-existed Sudan I and II in chili powders by the presented tactic is a great challenge and is not achieved in the present study.

## 4 Conclusion

This study observed the AIE phenomena of two synthetic Sudan dyes in solid matrices for the first time and achieved the rapid authentication of the adulteration of chili powders with two Sudan dyes by the combination of FFSFS and a simple PLSR algorithm. Although the quantitative result is not satisfactory, especially in the respect of sensitivity and detection limits, it can be effective as a convenient screening method for large quantity adulteration. More importantly, the results demonstrate that AIE-based FFSFS provides a new route for the application of fluorescence. Though the proposed method is not applicable for routine testing of chili powders because of its low sensitivity and high detection limits, the presented findings may provide a good basis for further investigations. Depending on the AIE mechanism, it may be not suitable for accurate and sensitive detection of low quantity targets. The most noteworthy merit of the strategy is the enhanced high selectivity of AIE based fluorescence spectroscopy in solid state, and the simplicity and rapidity without complicated sample pretreatment. However, as FFSFS measurements are restricted to the sample surface, high homogeneity is required to reflect the bulk of the sample and reduce the measurement error [41]. The successful employment of FFSFS for highly sensitive detection of low quantity components in food is still a challenge and merits further investigation. The relatively large measurement error of FFSFS toward solid samples proves to be problematic. In this work, we found that the sample moisture and particle size could influence the measurement error. In a previous study on the classification of cereal flours by FFSFS, some large in-group variances were also reported to originate from the differences in particle size and moisture [42]. To circumvent this limitation, it is necessary to thoroughly investigate the factors influencing measurement error, reveal the exact influence mechanism and reduce it as much as possible. Tutorials to diminish measurement error and practical methods of high precision are badly needed.

## Declarations

**Funding** The authors declare that no funds, grants, or other support were received during the preparation of this manuscript.

**Competing Interests** The authors have no relevant financial or non-financial interests to disclose.

**Author Contributions** All authors contributed to the study conception and design. Material preparation, data collection and analysis were performed by Zhao-Xi Liu. The first draft of the manuscript was written by Jin Tan and all authors commented on previous versions of the manuscript. All authors read and approved the final manuscript.

**Data Availability** The datasets generated during the current study are available from the corresponding author on reasonable request.

**Ethics approval** Not applicable.

**Consent to Participate** Not applicable.

**Consent for Publication** Not applicable.

## References

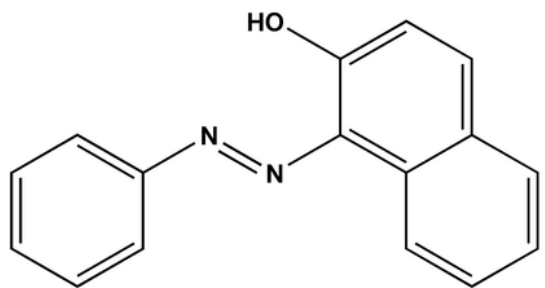
1. Karoui R, Blecker C (2011) Fluorescence spectroscopy measurement for quality assessment of food systems—a review. *Food Bioprocess Tech* 4(3):364–386. <https://doi.org/10.1007/s11947-010-0370-0>
2. Lenhardt L, Zeković I, Dramićanin T, Dramićanin MD, Bro R (2014) Determination of the botanical origin of honey by front-face synchronous fluorescence spectroscopy. *App Spectrosc* 68(5):557–563. <https://doi.org/10.1366/13-07325>
3. Hassoun A, Karoui R (2015) Front-face fluorescence spectroscopy coupled with chemometric tools for monitoring fish freshness stored under different refrigerated conditions. *Food Control* 54:240–249. <http://dx.doi.org/10.1016/j.foodcont.2015.01.042>
4. Danezis GP, Tsagkaris AS, Brusica V, Georgiou CA (2016) Food authentication: state of the art and prospects. *Curr Opin Food Sci* 10:22–31. <http://dx.doi.org/10.1016/j.cofs.2016.07.003>
5. Danezis GP, Tsagkaris AS, Camin F, Brusica V, Georgiou CA (2016) Food authentication: techniques, trends & emerging approaches. *Trac-Trend Anal Chem* 85:123–132. <https://doi.org/10.1016/j.trac.2016.02.026>
6. Włodarska K, Pawlak-Lemańska K, Khmelinskii I, Sikorska E (2017) Screening of antioxidant properties of the apple juice using the front-face synchronous fluorescence and chemometrics. *Food Anal Method* 10(5):1582–1591. <https://doi.org/10.1007/s12161-016-0711-3>
7. Włodarska K, Khmelinskii I, Sikorska E (2018) Authentication of apple juice categories based on multivariate analysis of the synchronous fluorescence spectra. *Food Control* 86:42–49. <https://doi.org/10.1016/j.foodcont.2017.11.004>
8. Boughattas F, Le Fur B, Karoui R (2019) Identification and quantification of tuna species in canned tunas with sunflower medium by means of a technique based on front face fluorescence spectroscopy (FFFS). *Food Control* 101:17–23. <https://doi.org/10.1016/j.foodcont.2019.02.003>
9. Boughattas F, Le Fur B, Karoui R (2019) Non-targeted identification of brine covered canned tuna species using front-face fluorescence spectroscopy combined with chemometric tools. *Food Anal Method* 12(12):2823–2834. <https://doi.org/10.1007/s12161-019-01638-w>
10. Cabrera-Bañegil M, Valdés-Sánchez E, Moreno D, Airado-Rodríguez D, Durán-Merás I (2019) Front-face fluorescence excitation-emission matrices in combination with three-way chemometrics for the

- discrimination and prediction of phenolic response to vineyard agronomic practices. *Food Chem* 270:162–172. <https://doi.org/10.1016/j.foodchem.2018.07.071>
11. Nhouchi Z, Botosoa EP, Chene C, Karoui R (2019) Potentiality of front-face fluorescence and mid-infrared spectroscopies coupled with partial least square regression to predict lipid oxidation in pound cakes during storage. *Food Chem* 275:322–332. <https://doi.org/10.1016/j.foodchem.2018.09.062>
  12. Sikorska E, Wójcicki K, Kozak W, Gliszczyńska-Świgło A, Khmelinskii I, Górecki T, Caponio F, Paradiso VM, Summo C, Pasqualone A (2019) Front-face fluorescence spectroscopy and chemometrics for quality control of cold-pressed rapeseed oil during storage. *Foods* 8(12):665. <https://doi.org/10.3390/foods8120665>
  13. Liu H, Ji Z, Liu X, Shi C, Yang X (2020) Non-destructive determination of chemical and microbial spoilage indicators of beef for freshness evaluation using front-face synchronous fluorescence spectroscopy. *Food Chem* 321:126628. <https://doi.org/10.1016/j.foodchem.2020.126628>
  14. Luo J, Xie Z, Lam JWY, Cheng L, Chen H, Qiu C, Kwok HS, Zhan X, Liu Y, Zhu D, Tang BZ (2001) Aggregation-induced emission of 1-methyl-1,2,3,4,5-pentaphenylsilole. *Chem Commun* 18:1740–1741. <https://doi.org/10.1039/b105159h>
  15. He X, Xiong LH, Huang Y, Zhao Z, Wang Z, Lam JWY, Kwok RTK, Tang BZ (2020) AIE-based energy transfer systems for biosensing, imaging, and therapeutics. *Trac-Trend Anal Chem* 122:115743. <https://doi.org/10.1016/j.trac.2019.115743>
  16. Li J, Wang J, Li H, Song N, Wang D, Tang BZ (2020) Supramolecular materials based on AIE luminogens (AIEgens): construction and applications. *Chem Soc Rev* 49(4):1144–1172. <https://doi.org/10.1039/c9cs00495e>
  17. Niu G, Zhang R, Shi X, Park H, Xie S, Kwok RTK, Lam JWY, Tang BZ (2020) AIE luminogens as fluorescent bioprobes. *Trac-Trend Anal Chem* 123:115769. <https://doi.org/10.1016/j.trac.2019.115769>
  18. Jiang Y, Zhong Z, Ou W, Shi H, Alam P, Tang BZ, Qin J, Tang Y (2020) Semi-quantitative evaluation of seafood spoilage using filter-paper strips loaded with an aggregation-induced emission luminogen. *Food Chem* 327:127056. <https://doi.org/10.1016/j.foodchem.2020.127056>
  19. Xu L, Ni L, Zeng F, Wu S (2020) Tetranitrile-anthracene as a probe for fluorescence detection of viscosity in fluid drinks via aggregation-induced emission. *Analyst* 145(3):844–850. <https://doi.org/10.1039/C9AN02157D>
  20. Li YY, Hou LY, Shan FJ, Zhang ZL, Li YJ, Liu YQ, Peng QC, He J, Li K (2019) Novel aggregation-induced emission luminogen based molecularly imprinted fluorescence sensor for ratiometric determination of Rhodamine B in food samples. *ChemistrySelect* 4:11256–11261. <https://doi.org/10.1002/slct.201903141>
  21. Mazzetti M, Fascioli R, Mazzoncini I, Spinelli G, Morelli I, Bertoli A (2004) Determination of 1-phenylazo-2-naphthol (Sudan I) in chilli powder and in chilli-containing food products by GPC clean-

- up and HPLC with LC/MS confirmation. *Food Addit Contam A* 21(10):935–941.  
<https://doi.org/10.1080/02652030400007252>
22. Cornet V, Govaert Y, Moens G, Van Loco J, Degroodt JM (2006) Development of a fast analytical method for the determination of Sudan dyes in chili- and curry-containing foodstuffs by high-performance liquid chromatography-photodiode array detection. *J Agric Food Chem* 54(3):639–644.  
<https://doi.org/10.1021/jf0517391>
  23. Di Anibal CV, Odena M, Ruisánchez I, Callao MP (2009) Determining the adulteration of spices with Sudan I-II-IV dyes by UV–visible spectroscopy and multivariate classification techniques. *Talanta* 79(3):887–892. <https://doi.org/10.1016/j.talanta.2009.05.023>
  24. Di Anibal CV, Ruisánchez I, Callao MP (2011) High-resolution  $^1\text{H}$  Nuclear Magnetic Resonance spectrometry combined with chemometric treatment to identify adulteration of culinary spices with Sudan dyes. *Food Chem* 124(3):1139–1145. <https://doi.org/10.1016/j.foodchem.2010.07.025>
  25. Di Anibal CV, Ruisánchez I, Fernández M, Forteza R, Cerdà V, Callao MP (2012) Standardization of UV–visible data in a food adulteration classification problem. *Food Chem* 134(4):2326–2331.  
<http://dx.doi.org/10.1016/j.foodchem.2012.03.100>
  26. Di Anibal C, Rodriguez MS, Albertengo L (2014) UV-visible spectroscopy and multivariate classification as a screening tool to identify adulteration of culinary spices with Sudan I and blends of Sudan I + IV dyes. *Food Anal Method* 7(5):1090–1096. <https://doi.org/10.1007/s12161-013-9717-2>
  27. Di Anibal CV, Rodríguez MS, Albertengo L (2015) Synchronous fluorescence and multivariate classification analysis as a screening tool for determining Sudan I dye in culinary spices. *Food Control* 56:18–23. <http://dx.doi.org/10.1016/j.foodcont.2015.03.010>
  28. Haughey SA, Galvin-King P, Ho YC, Bell SEJ, Elliott CT (2015) The feasibility of using near infrared and Raman spectroscopic techniques to detect fraudulent adulteration of chili powders with Sudan dye. *Food Control* 48:75–83. <https://doi.org/10.1016/j.foodcont.2014.03.047>
  29. Márquez C, Ruisánchez I, Callao MP (2019) Qualitative and quantitative multivariate strategies for determining paprika adulteration with Sudan I and II dyes. *Microchem J* 145:686–692.  
<https://doi.org/10.1016/j.microc.2018.11.034>
  30. Andoh SS, Nyave K, Asamoah B, Kanyathare B, Nuutinen T, Mingle C, Peiponen KE, Roussey M (2020) Optical screening for presence of banned Sudan III and Sudan IV dyes in edible palm oils. *Food Addit Contam A* 37(7):1049–1060. <https://doi.org/10.1080/19440049.2020.1726500>
  31. Monago-Maraña O, Eskildsen CE, de la Peña AM, Galeano-Díaz T, Wold JP (2020) Non-destructive fluorescence spectroscopy combined with second-order calibration as a new strategy for the analysis of the illegal Sudan I dye in paprika powder. *Microchem J* 154:104539.  
<https://doi.org/10.1016/j.microc.2019.104539>
  32. Wu CY, Lu QJ, Miu XR, Fang AJ, Li HT, Zhang YY (2018) A simple assay platform for sensitive detection of Sudan I–IV in chilli powder based on CsPbBr<sub>3</sub> quantum dots. *J Food Sci Tech* 55:2497–2503. <https://doi.org/10.1007/s13197-018-3167-1>

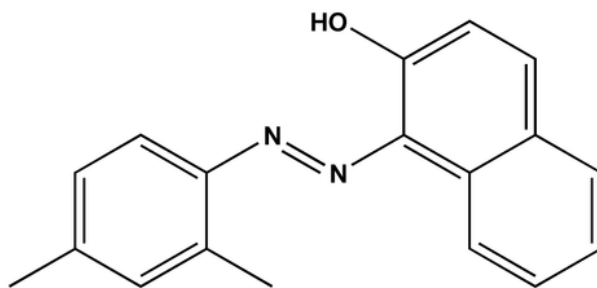
33. Hansen GJT, Almonacid J, Albertengo L, Rodriguez MS, Di Anibal C, Delrieux C (2019) NIR-based Sudan I to IV and Para-Red food adulterants screening. *Food Addit Contam A* 36(8):1163–1172. <https://doi.org/10.1080/19440049.2019.1619940>
34. Yoon Y, Jo S, Park SJ, Kim HM, Kim D, Lee TS (2019) Unusual fluorescence of *o*-phenylazonaphthol derivatives with aggregation-induced emission and their use in two-photon cell imaging. *Chem Commun* 55(47):6747–6750. <https://doi.org/10.1039/C9CC03106E>
35. Dankowska A, Kowalewski W (2019) Comparison of different classification methods for analyzing fluorescence spectra to characterize type and freshness of olive oils. *Eur Food Res Technol* 245(3):745–752. <https://doi.org/10.1007/s00217-018-3196-z>
36. Dankowska A, Kowalewski W (2019) Tea types classification with data fusion of UV–vis, synchronous fluorescence and NIR spectroscopies and chemometric analysis. *Spectrochim Acta A* 211:195–202. <https://doi.org/10.1016/j.saa.2018.11.063>
37. Sikorska E, Wlodarska K, Khmelinskii I (2020) Application of multidimensional and conventional fluorescence techniques for classification of beverages originating from various berry fruit. *Methods Appl Fluores* 8:015006. <https://doi.org/10.1088/2050-6120/ab6367>
38. Hong Y, Lam JWY, Tang BZ (2011) Aggregation-induced emission. *Chem Soc Rev* 40:5361–5388. <https://doi.org/10.1039/C1CS15113D>
39. Mei J, Leung NLC, Kwok RTK, Lam JWY, Tang BZ (2015) Aggregation-induced emission: together we shine, united we soar! *Chem Rev* 115:11718–11940. <https://doi.org/10.1021/acs.chemrev.5b00263>
40. Sharma S, Sarika Bharti A, Singh R, Uttam KN (2019) Non-destructive phenotyping of chili pepper ripening using spectroscopic probes: a potential approach for shelf-life measurement. *Anal Lett* 52(10):1590–1613. <https://doi.org/10.1080/00032719.2018.1558231>
41. Sikorska E, Khmelinskii I, Sikorski M (2019) Fluorescence spectroscopy and imaging instruments for food quality evaluation. In: Zhong J, Wang X (eds) *Evaluation technologies for food quality*. Woodhead Publishing, Cambridge(MA), pp 491–533. <https://doi.org/10.1016/B978-0-12-814217-2.00019-6>
42. Zeković I, Lenhardt L, Dramićanin T, Dramićanin MD (2012) Classification of intact cereal flours by front-face synchronous fluorescence spectroscopy. *Food Anal Method* 5(5):1205–1213. <https://doi.org/10.1007/s12161-011-9359-1>

## Figures



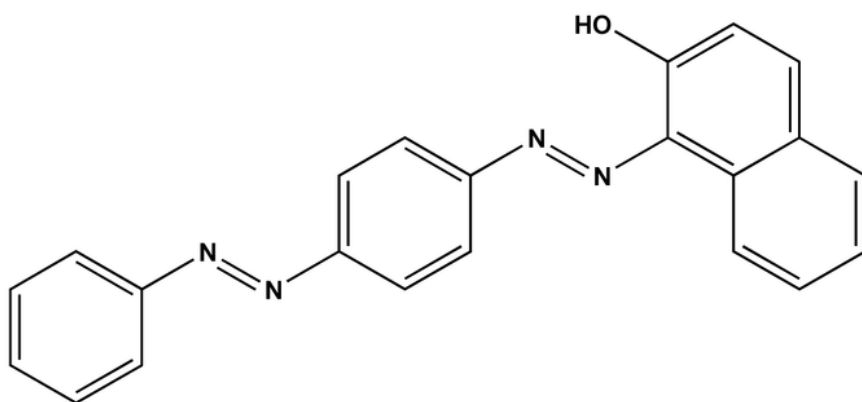
**1-phenylazo-2-naphthalenol**

**Sudan I**



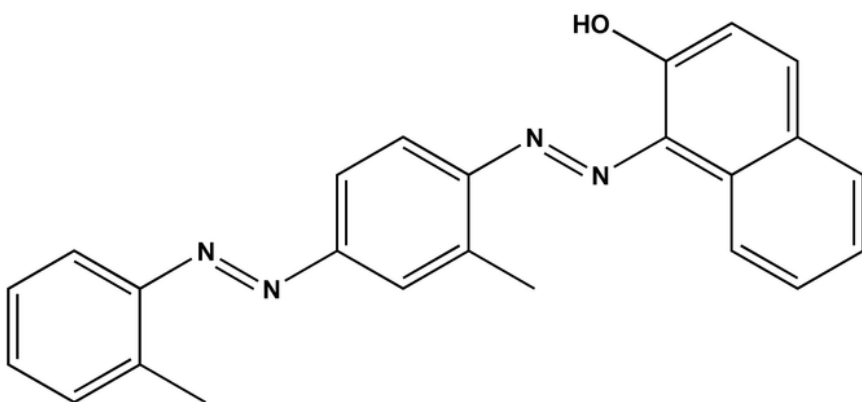
**1-[(2,4-dimethylphenyl)azo]-2-naphthalenol**

**Sudan II**



**1-[4-(phenylazo)phenyl]azo-2-naphthalenol**

**Sudan III**



**1-2-methyl-4-[(2-methylphenyl)azo]phenylazo-2-naphthalenol**

**Sudan IV**

**Figure 1**

Chemical structures of four Sudan dyes (Sudan I-IV).

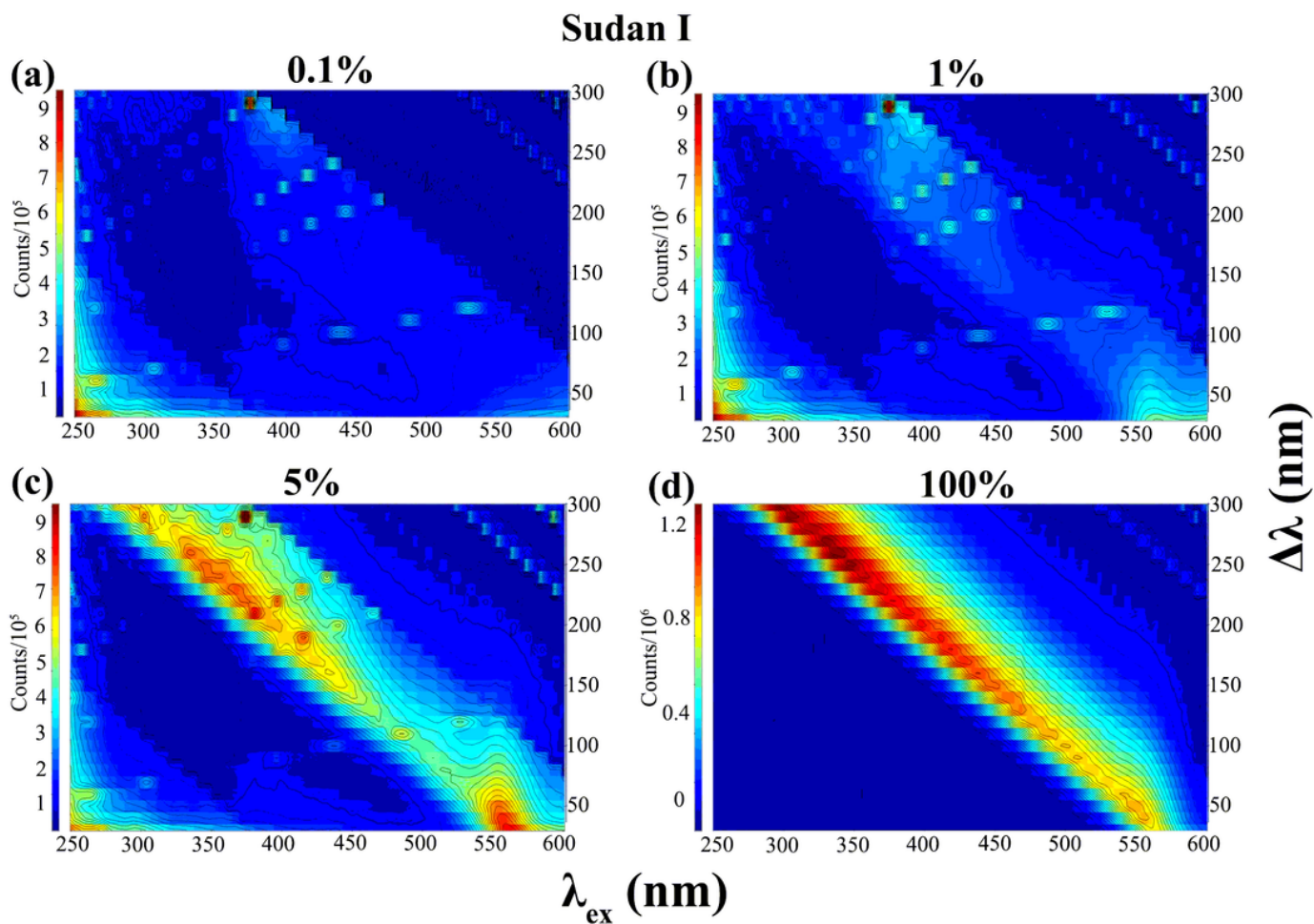


**Figure 2**

Total front-face synchronous fluorescence spectra of pure Sudan I and its solid solutions of different concentrations (w%) in BaSO<sub>4</sub>.

## Sudan II

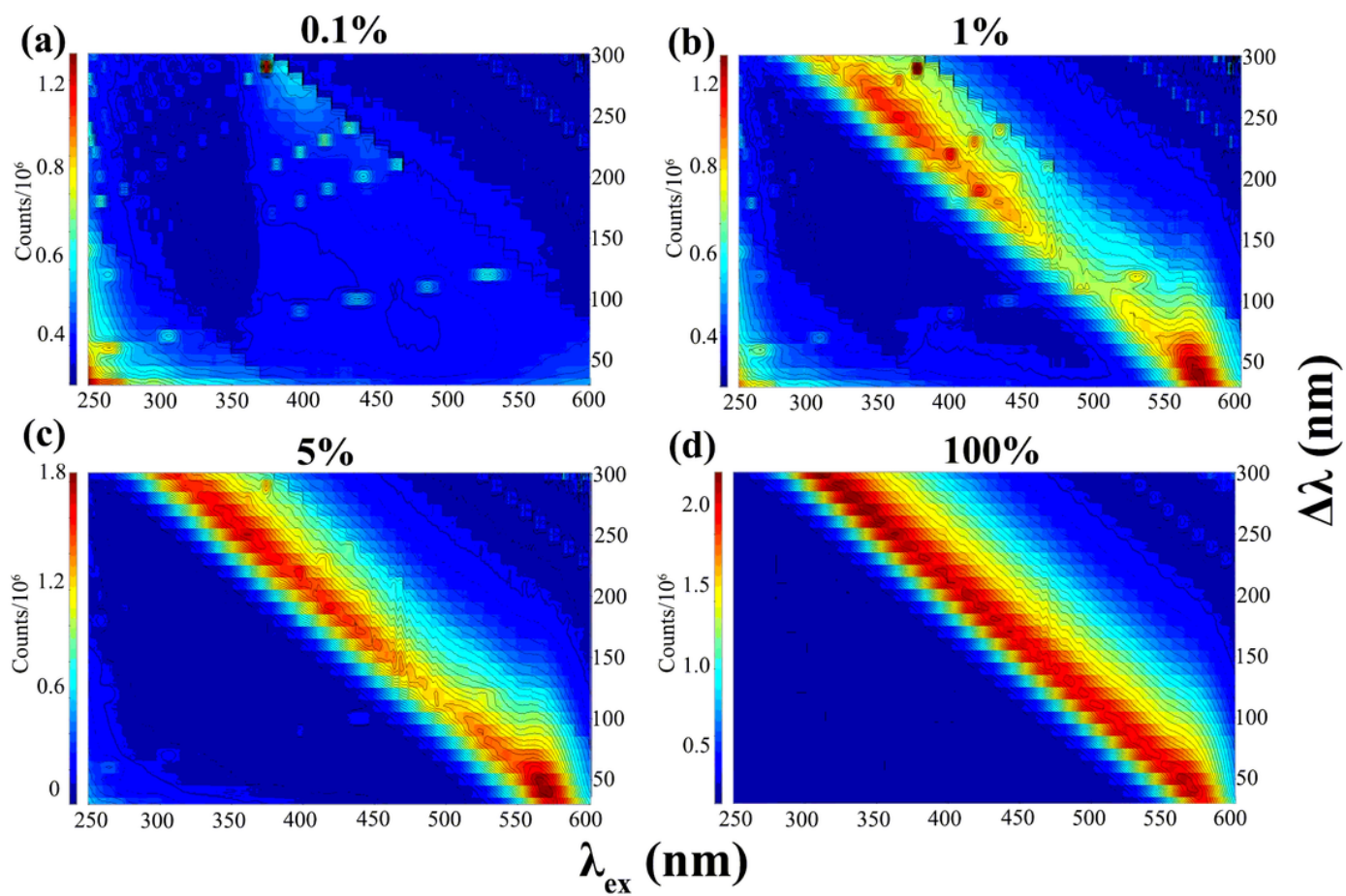
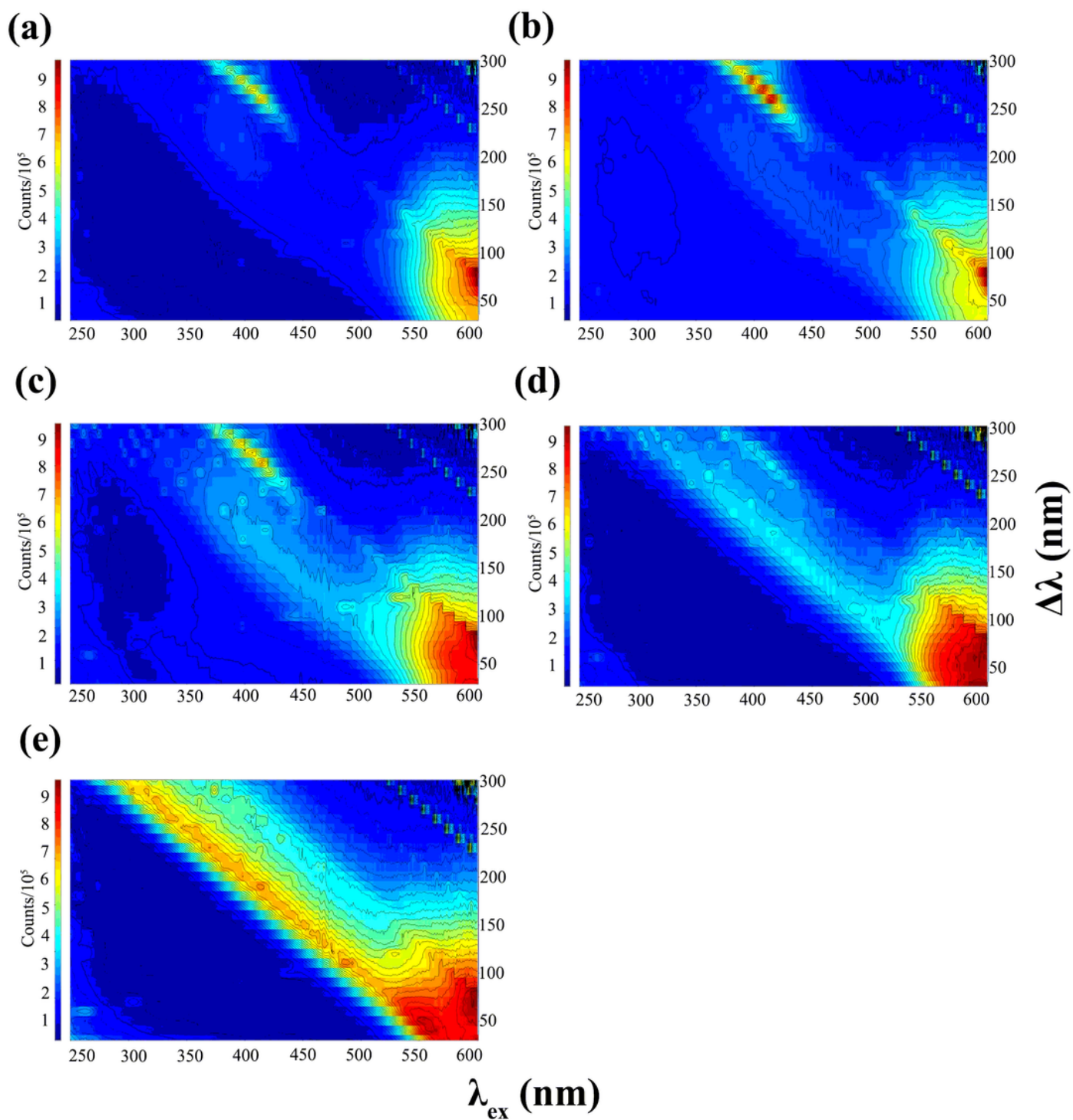


Figure 3

Total front-face synchronous fluorescence spectra of pure Sudan II and its solid solutions of different concentrations (w%) in  $\text{BaSO}_4$ .



**Figure 4**

Total front-face synchronous fluorescence spectra of three typical chili powders without Sudan dye adulteration (a, b and c) and one of the chili powders adulterated with 1% (w%) Sudan I or Sudan II (d, +1% Sudan I; e, +1% Sudan II).

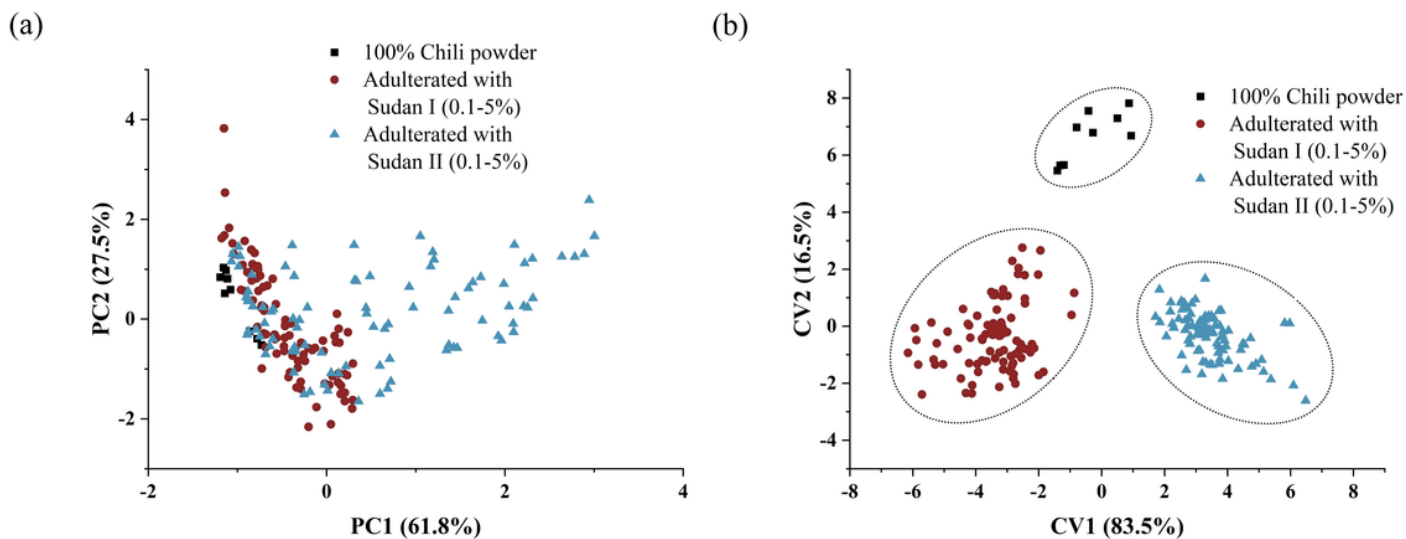


**Figure 5**

PCA (a) and LDA (b) score plots for the discrimination of unadulterated chili powders and chili powders adulterated with Sudan I or Sudan II (0.1-5%, w%) based on the front-face synchronous fluorescence spectra at  $\Delta\lambda = 180$  nm.

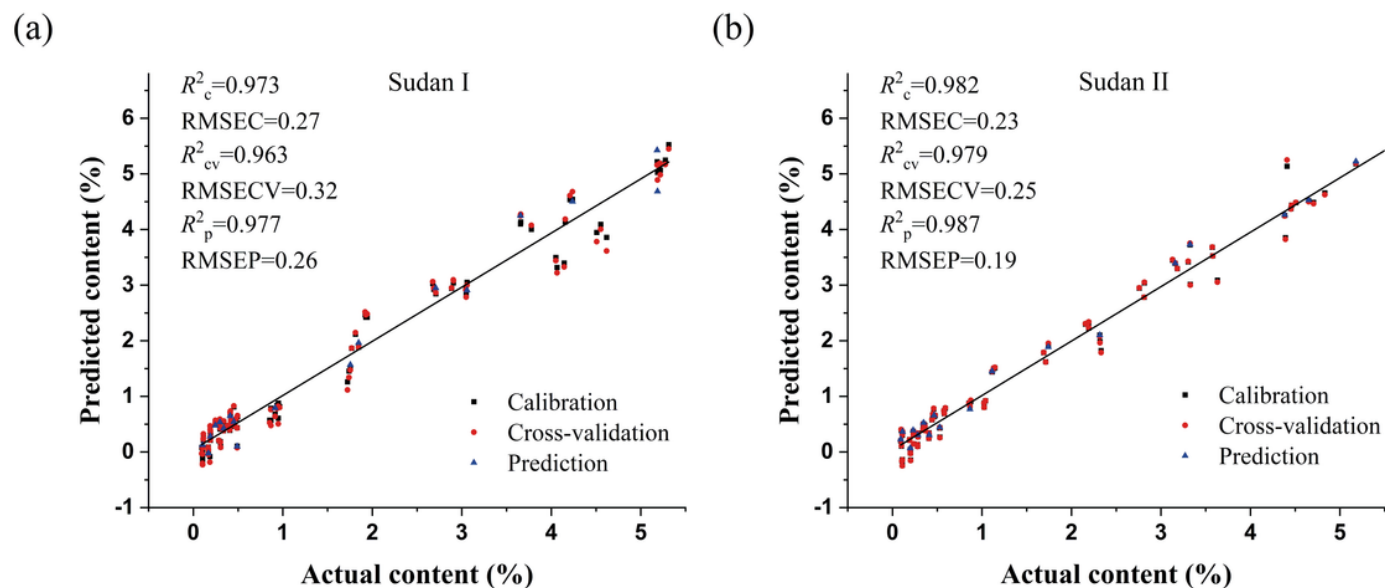


**Figure 6**

PLSR predicted versus actual contents (determined by HPLC) of Sudan I (a) and Sudan II (b) in chili powders based on the front-face synchronous fluorescence spectra under optimal conditions as shown in Table 1. The cross-validation shown in the figures is full (*leave-one-out*) cross-validation.

## Supplementary Files

This is a list of supplementary files associated with this preprint. Click to download.

- [Graphicalabstract.tif](#)